Engineering Geology 123 (2011) 235–245

Contents lists available at SciVerse ScienceDirect

Engineering Geology

journal homepage: www.elsevier.com/locate/enggeo

Geotechnical reconnaissance and liquefaction analyses of a liquefaction site with silty fine sand in Southern Taiwan

Wen-Jong Chang [a,*], Sheng-Huoo Ni [a], An-Bin Huang [b], Yan-Hong Huang [a], Yu-Zhang Yang [a]

[a] Department of Civil Engineering, National Cheng Kung University, Tainan 70101, Taiwan
[b] Department of Civil Engineering, National Chiao Tung University, Hsinchu 300, Taiwan

ARTICLE INFO

Article history:
Received 25 October 2010
Received in revised form 1 August 2011
Accepted 4 September 2011
Available online 19 September 2011

Keywords:
Soil liquefaction
Fines content
Silty sand
Case history

ABSTRACT

Geotechnical reconnaissance of a recurrent liquefaction site at a Quaternary alluvial deposit in southern Taiwan was conducted to establish a comprehensive case history for liquefaction on silty fine sand with high fines content. The liquefaction occurred at a silty fine sand layer with $D_{50} = 0.09$ mm and fines content greater than 35% and was triggered by a $M_w = 6.4$ earthquake on March 4, 2010, which induced maximum horizontal acceleration up to 0.189 g at the site. In situ subsurface characterizations, including standard penetration test, cone penetration test, and shear wave velocity measurement, were performed as well as cyclic simple shear tests on undisturbed specimens retrieved by a modified hydraulic piston sampler. Comparisons of cyclic resistance ratios (CRRs) indicate that CPT sounding with standard penetration rate could overestimate the resistance ratio and drainage conditions during penetration should be considered for high fines content soil in the liquefaction analysis. Additionally, variations of CRRs from different in situ tests indicate that correlations among in situ tests and CRR could be soil specific and precautions should be taken when using these curves on silty fine sands.

1. Introduction

The Jiasian earthquake ($M_w = 6.4$) occurred at 8:18 local time on 4 March 2010 with the epicenter 17 km southeast of Jiasian Township in Kaohsiung County, Southern Taiwan, and was the biggest earthquake in the Kaohsiung area since 1900. The seismic event caused 64 injuries and over 340 buildings were damaged. In addition, the strong ground motion de-railed two wheels of a Taiwan High Speed Rail (THSR) train and the THSR service was suspended for two days.

Sand boils from soil liquefaction were observed in Sinhua Township, which is about 40 km away from the epicenter. Sand boil crests were randomly spread within a 350 m long and 250 m wide paddy field, as shown in Fig. 1, and this soil liquefaction site is named the Sinhua site hereafter. The position of the sand boil zone in relation to the THSR railway and the typical sand boil pattern in the Sinhua site are shown in Fig. 2. Each sand boil has several aligned vents and the ejected sand is mainly grey fine sands with yellowish brown silts. The pore pressure dissipation process lasted at least 36 hours, and a significant amount of water was squeezed out after the earthquake, causing significant soaking at nearby surface and a rise of water level in the irrigation channels.

The Sinhua site has four significant features that deserve more detailed study. First, the sand boil spots by the 2010 Jiasian earthquake overlapped with the locations of soil liquefaction in the 1946 Sinhua earthquake, which was triggered by the slip of Sinhua fault, only 1.5 km from the Sinhua site. This recurrence provides an opportunity to study the geologic and geotechnical conditions for the recurrence of soil liquefaction. Second, sand boils were observed only on east side of the THSR elevated railway, although soil liquefaction occurred on both sides of THSR railway in the 1946 Sinhua earthquake. Because the THSR piers are supported by 60 m piles with 30 m spacing, the pile rows may have created a wave propagating boundary at a shallow depth. Consequently, dynamic soil-structure interactions are likely to play an important role in altering the ground shaking and subsequently triggering the liquefaction. Third, pre-earthquake boring logs conducted four months before the Jiasian earthquake are available at the Sinhua site, which provides a case to study the variation of subsurface conditions after liquefaction. Finally, the soil stratums in this liquefied layers show fines content of over 35% and the site provides a case history to verify liquefaction evaluation techniques in high fines content soils.

Due to these above mentioned features, geotechnical reconnaissance was conducted two days after the earthquake. The subsurface characterization work included standard penetration tests (SPT) with split tube sampling, seismic cone penetration tests with pore pressure measurement (SCPTu), multichannel analysis of surface waves (MASW), and cyclic simple shear tests on undisturbed specimens by a modified hydraulic piston sampler. This paper presents the preliminary geotechnical reconnaissance results with a focus on the engineering properties related to soil liquefaction. Additionally,

* Corresponding author. Tel.: +886 6 2757575 63128; fax: +886 6 2358548.
E-mail address: wjchang@mail.ncku.edu.tw (W.-J. Chang).

0013-7952/$ – see front matter © 2011 Elsevier B.V. All rights reserved.
doi:10.1016/j.enggeo.2011.09.003

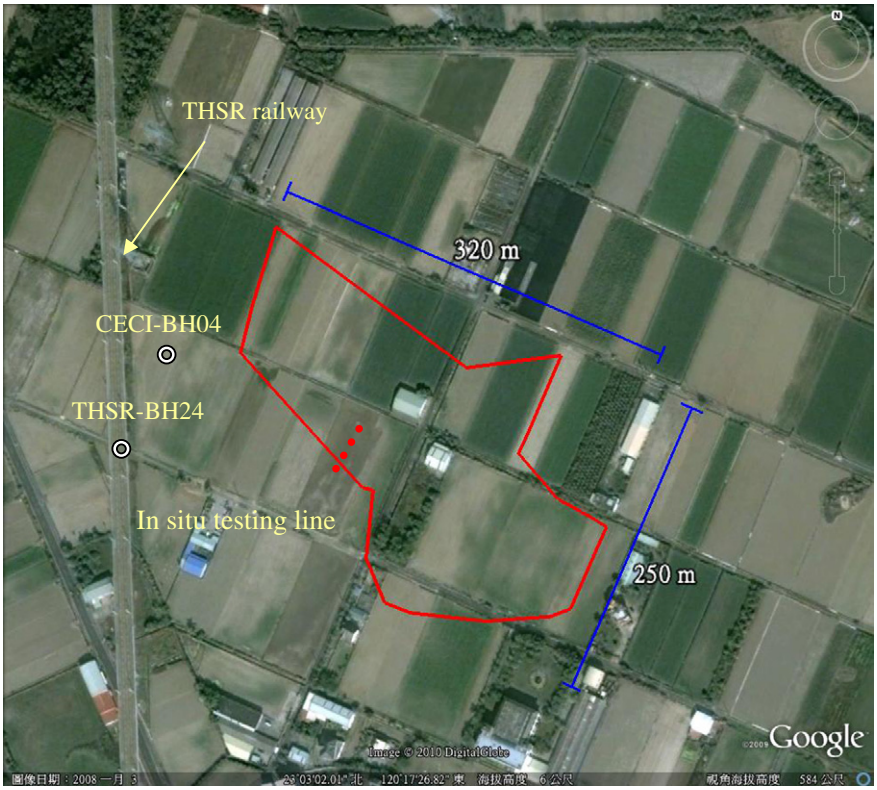

Fig. 1. Extent of sand boil in Sinhua site, pre-earthquake boring logs, and in situ testing line.

empirical correlations and laboratory testing results are implemented to assess the liquefaction resistance of the site and comparisons are conducted to evaluate the applicability of the empirical correlations on high fines content soil.

2. Geologic setting and historical liquefaction

Fig. 3 shows the geological setting of the Sinhua site, sand boil locations in the 1946 Sinhua earthquake ($M_s = 6.1$) (Chang et al., 1947) and after the 2010 Jiasian earthquake. With regard to regional geology, the western side of Taiwan is stratigraphically known as a western foothills province covered by flood plains and terrace deposits. The Sinhua site is located on one of the flood plains named the Tainan plain, and the geologic categorization is Quaternary alluvium in the Central Geologic Survey (CGS) geological map. The alluvial deposits are composed of clay, silt, sand, and gravel, with a soil thickness of over 100 m. The rock formations beneath the alluvial deposits are dominated by alternations of sandstone and shale or mudstone (CGS, 2005). The eastern rim of the Tainan plain is a Holocene terrace deposit, which represents cycles of marine transgression and regression on the eastern rim of plain. The rock formation below the Holocene terrace deposit is generally termed the Toukoshan formation, and is composed of sandstone, mudstone, and shale.

The distribution of sand boils from the 1946 Sinhua earthquake is shown in Fig. 3. The 1946 Sinhua earthquake was triggered by slips of Sinhua fault that extends about 6 km in the N80°E direction, and the epicenter was located at 23.1°N, 120.3°E at a depth of 5 km. The ground shaking intensity in the Sinhua area was level V (strong) in Central Weather Bureau (CWB) intensity scale, which represents ground acceleration from 0.080 to 0.250 g. Chang et al. (1947) reported that the ejected soil was fine sand with high fines content from a shallow depth, based on visual comparisons of the ejected soil and a nearby river bank profile.

The locations of sand boil in the 2010 Jiasian earthquake are also shown in Fig. 3. Sand boil crests were observed in two zones, the larger one on the west side of the Sinhua fault, and the other in an alluvial deposit by two streams on the Sinhua fault. The overlap of sand boil locations in the 1946 and 2010 earthquakes shows the recurrence of liquefaction of this area when subjected to moderate to strong ground shaking. In addition, the occurrence of sand boils only on the east side of the THSR railway in the 2010 earthquake indicates that the construction of 60 m deep piles may affect the triggering of liquefaction.

3. Seismicity and ground motion

The focus of the 2010 Jiasian earthquake was located at 22.97°N, 120.71°E at a depth of 22.6 km (CWB). According to a preliminary investigation by Institute of Earth Science Academia Sinica based on global seismic network data, the earthquake was triggered by a blind thrust fault with a northwest–southeast (318°) strike, dipping toward the east (41°), with a maximum slip of 50 cm (Lee and Lui, 2010).

The Sinhua site was 44 km away from the epicenter and categorized as a level V area on the CWB intensity scale during the 2010 Jiasian earthquake. To estimate the local ground shaking characteristics, seismic records from four seismic stations within a 10 km radial distance centered on the Sinhua site were collected, and details of the stations are summarized in Table 1. The locations of seismic stations and geologic formations are shown in Fig. 4. Among the four stations, station CHY063 is located in the Toukoshan formation with a soil thickness of less than 3 m, and thus the record represents the outcrop motions of the hard stratum underlying the soil layers at the Sinhua site. The other three stations are located in Quaternary alluvium. Both CHY021 and CHY023 stations are located on the east side of the THSR railway, and the CHY078 station is on the west side. The

Fig. 2. Sand boils at Sinhua site (2010/03/05).

peak horizontal acceleration (PGA) in the vicinity of the Sinhua site is between 0.089 and 0.136 g.

Considering the geologic formation, distance to Sinhua site, and radial distance from the epicenter, the seismic record of station CHY021 is selected as the representative ground motion of the Sinhua site. The acceleration time histories and Fourier spectrum of the two stations are shown in Fig. 5. Comparisons of the peak ground accelerations between the two stations show that de-amplification effects occurred in the alluvium deposit. For subsequent analyses, the maximum ground acceleration (a_{max}) at the Sinhua site is estimated at 0.189 g from the geometric mean of horizontal accelerations.

The energy content for both stations is concentrated in the frequency range from 0.2 to 7.0 Hz. However, on the soft soil surface, the frequency corresponding to the maximum Fourier amplitude reduces from 0.8 to 0.45 Hz in the NS component, and from 1.0 to 0.4 Hz in the EW component, which indicates that the wave propagating behavior within the soil stratum was nonlinear. The Arias durations, defined as the duration between 5 and 95% normalized Aria intensity, of station CHY021 were 25.5 s and 20.8 s for NS and EW components, respectively.

4. Subsurface characterization

Subsurface site characterizations to establish a comprehensive case history for liquefaction analyses were initiated two days after the earthquake. The investigation program included documentation of sand boil features, collection of previous boring logs, in situ site characterization tests, and laboratory tests. To perform stress approaches for liquefaction evaluation with various in situ properties, three in situ site characterization techniques were conducted, including standard penetration tests (SPT) with split tube sampling, cone penetration tests with pore pressure measurement and downhole testing (SCPTu), and multichannel analysis of surface waves (MASW). All the tests were conducted along the testing line marked in Fig. 1. Additionally, undisturbed soil samples were retrieved with a modified hydraulic piston sampler for dynamic laboratory tests.

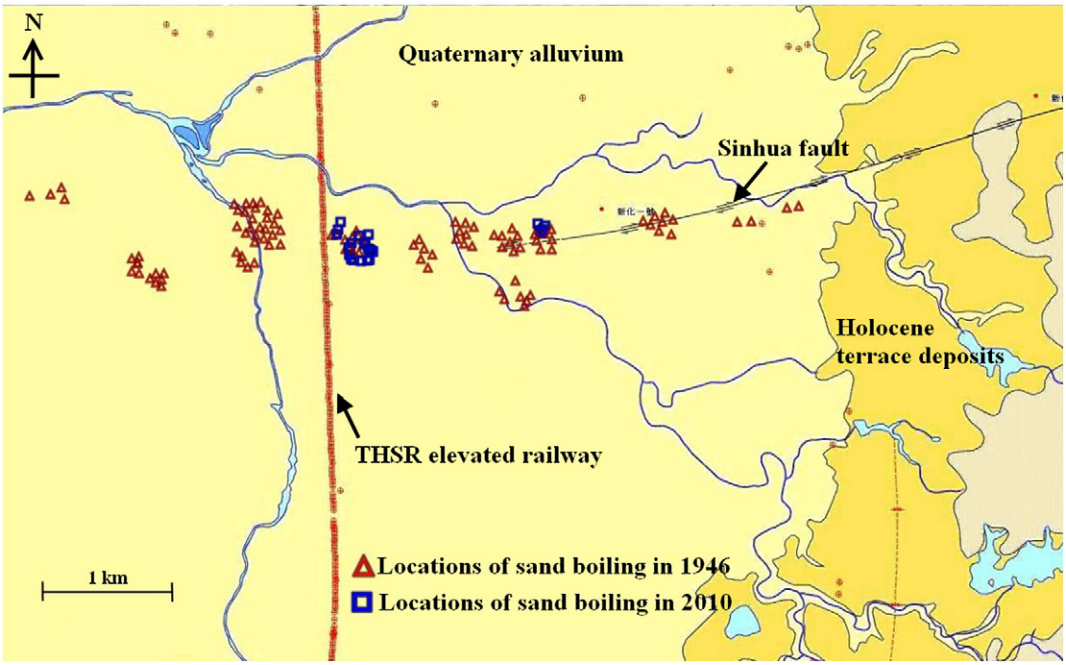

Fig. 3. Geologic setting and sand boil locations of 1946 and 2010 earthquakes.
(Compiled from CGS, 2005; Chang et al., 1947).

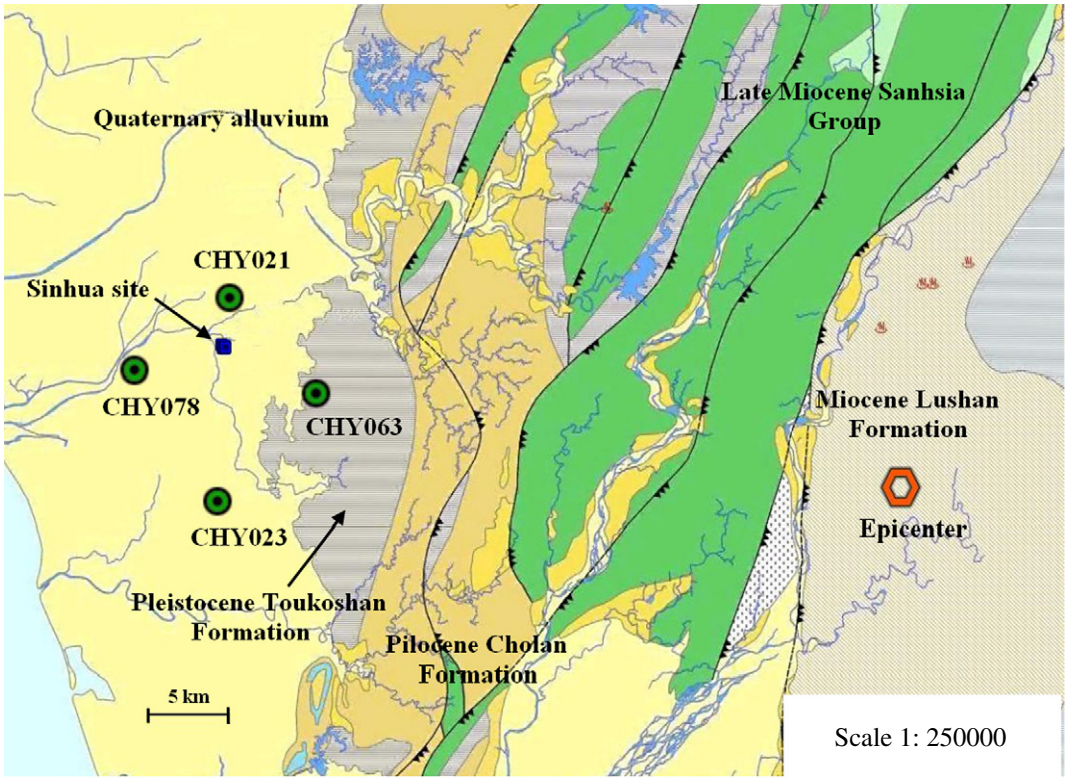

Fig. 4. Locations of nearby seismic stations and geologic formations. (Modified from CGS, 2010).

4.1. Borehole data

Two borehole logs (THSR-BH24 and CECI-BH04) are presented to show the pre-earthquake soil strata, and the locations of the two boreholes are shown in Fig. 1. The two borehole logs, as shown in Fig. 6, were conducted for previous construction projects in the proximity of Sinhua site. The THSR-BH24 borehole log, acquired from Database Integrated Construction Project of CGS, was conducted in 1993 for the THSR pile-supported railway and located 100 m away from the closest sand boil spot. The soil stratum for the top 20 m are consisted of sandy clay, clayey sand, and fine sand with SPT-N values (blow counts per foot in a standard penetration test) of less than 11. Below the soft cover layers, the intercalation of silty sand and silty clay extends to 70 m deep (the bottom of the borehole). For the intercalation strata, the average SPT-N value for silty clay is 20, and over 30 for silty sand. The CECI-BH04 borehole log was conducted in 2009 for a local road and located only 30 m away from the closest sand boil spot. This borehole data shows that the top 20 m is very soft, with SPT-N values from 3 to 7. In addition, a silty sand layer at a depth from 2.2 to 5.8 m has an average SPT-N value of 5 and is intercalated by silty clay layers. The ground water table in this area is generally less than 1.5 m from surface.

Table 1
Summary of seismic stations around the Sinhua site.

Station	Distance to epicenter (km)	Distance to Site (km)	MHA (gal) Vertical/NS/EW	Geologic formation
CHY063	37.6	6.4	71.2/ 174.7/ 385.2	Toukoushan formation
CHY021	44.1	3.2	57.4/ 136.1/ 130.9	Quaternary alluvium
CHY023	43.3	9.5	37.0/ 89.0/ 121.5	Quaternary alluvium
CHY078	49.1	5.9	25.3/ 61.5/ 101.7	Quaternary alluvium

Note: The epicenter distance for the Sinhua site is 44 km.

Although the distance between the two boreholes is only 80 m, the soil layer sequences of the top 20 m show slight differences in the elevation and thickness of the loose silty sand layer. To clarify the depth of the liquefied layers, another three boreholes were drilled right on the sand boil crests on the investigation line marked on Fig. 1. Among the three boreholes, one is for continuous SPT tests with split tube samples for physical property tests, and the other two are for retrieving undisturbed samples. The procedure of SPT complied with ASTM D1586 using a safety hammer with rope-cathead operation. According to Moh and Associates (2000), the energy ratio (ER) of SPT in west central Taiwan can be represented as:

$$ER(\%) = 30\frac{z}{11} + 50 \text{ for } z \leq 11 \quad (1a)$$

$$ER(\%) = 80 \text{ for } z > 11 \quad (1b)$$

where z is the depth from surface in meter. Although no energy measurement was conducted in this study, the SPT equipment, operation procedure, and soil layer in this area are similar to those cases reported in Moh and Associates (2000); therefore, the energy ratio expressed in Eq. (1) would be the best estimation.

The first borehole is named SLS (Sinhua liquefaction site), and the test results are shown in Table 2. The profiles of the SPT-N value, fines content (particle size<0.075 mm), and plasticity index (PI) from THSR-BH24, CECI-BH04, and SLS are compiled and plotted in Fig. 7. The borehole data from CECI-BH04 and SLS show that a silty fine sand layer at depths of 4 to 9 m is intercalated by two silty clay layers. The soil layer at depths from 20 to 33 m consists of hard silty sand with an SPT-N value greater than 30. Based on the data from THSR-BH24, intercalation among silty sand, silty clay, and clayey silt layers was found below 33 m. Considering the distance to liquefied zone and consistency of layer sequence, the CECI-BH04 and SLS logs represent the pre-earthquake and post-earthquake soil strata of the top 20 m

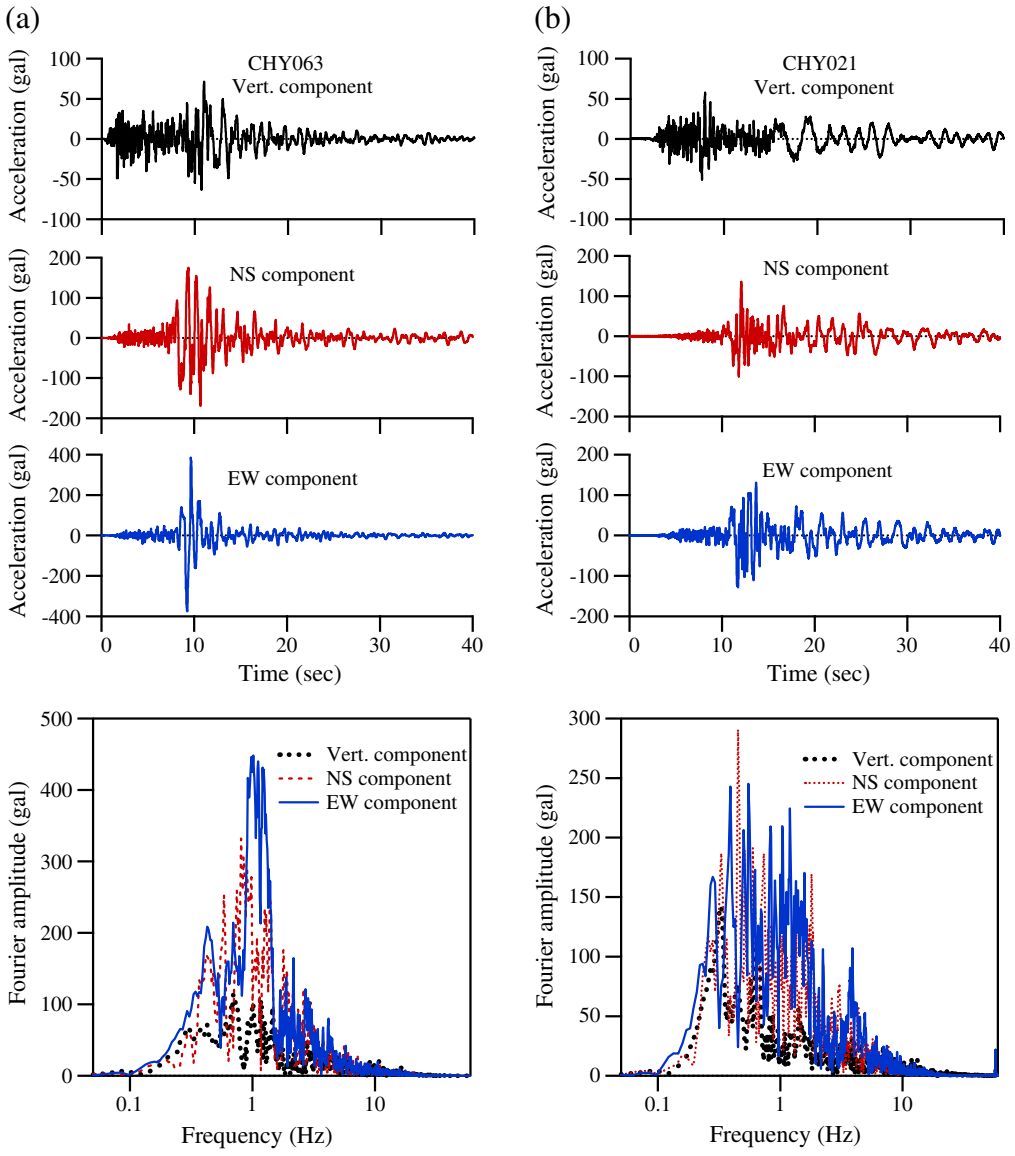

Fig. 5. Ground acceleration histories and Fourier spectrum: (a) on outcrop of hard stratum (CHY063), and (b) on surface of soft soil stratum (CHY021).

respectively, while the THSR-BH24 log represents the soil layers from 30 to 70 m in depth.

The ejected soil collected from the sand boil deposits is grey silty fine sand. In the preliminary stage of investigation, the silty fine sand interlayer at depths of 4 to 9 m was assumed as the liquefiable layer and evidences from the field investigations and laboratory tests show that the most critical layer is located at depths from 5 to 6 m. Comparisons of SPT-N values between the pre-earthquake log (CECI-BH04) and post-earthquake log (SLS) show that the average SPT-N values in the liquefiable silty fine sand layer (4–9 m) increased from 5 to 7.5 and the average fines content reduced from 60 to 35% after liquefaction (Fig. 7). Field observations at the Sinhua site show that liquefaction could change the soil properties in silty fine sand interlayer.

4.2. Cone penetration results

Two CPT soundings were performed located 1.5 m from the SLS borehole. The first CPT sounding was performed with a standard penetration rate at 20 mm per second (PR = 20 mm/s), and downhole shear wave velocity tests were conducted every meter. The second sounding was performed at a penetration rate of 1 mm/s (PR = 1 mm/s) to achieve drain condition during the penetration process for high fine content sandy soil (Kim et al., 2008). The CPT soundings for tip resistance (q_c), friction ratio ($R_f = f_s/q_c$, f_s = local friction), and pore pressure (Pw) are shown in Fig. 8 along with the soil layers from the SLS boring log.

The CPT soundings show that a low tip resistance layer exists from depths of 3 to 9 m, with a hard stratum below 20 m, which is consistent with the SPT boring logs. The soil behavior types from the UBC-1983 chart indicate that the soils at depths from 3 to 9 m are sandy silt to sand, and this layer is bounded by clayey silt or silty clay layers. The variations between the hydrostatic water pressure and pore pressure around the cone in the slow penetration test indicate that the excess pore pressure due to penetration dissipated quickly within depths of 3.5 to 9 m, and the above and below layers are less permeable. The soil type, tip resistance, and soil profile indicate that soils at depths from 4 to 9 m are liquefiable. Additionally, the confinement of the liquefiable layer by two less permeable layers explains that why the dissipation process lasted for over 36 hours.

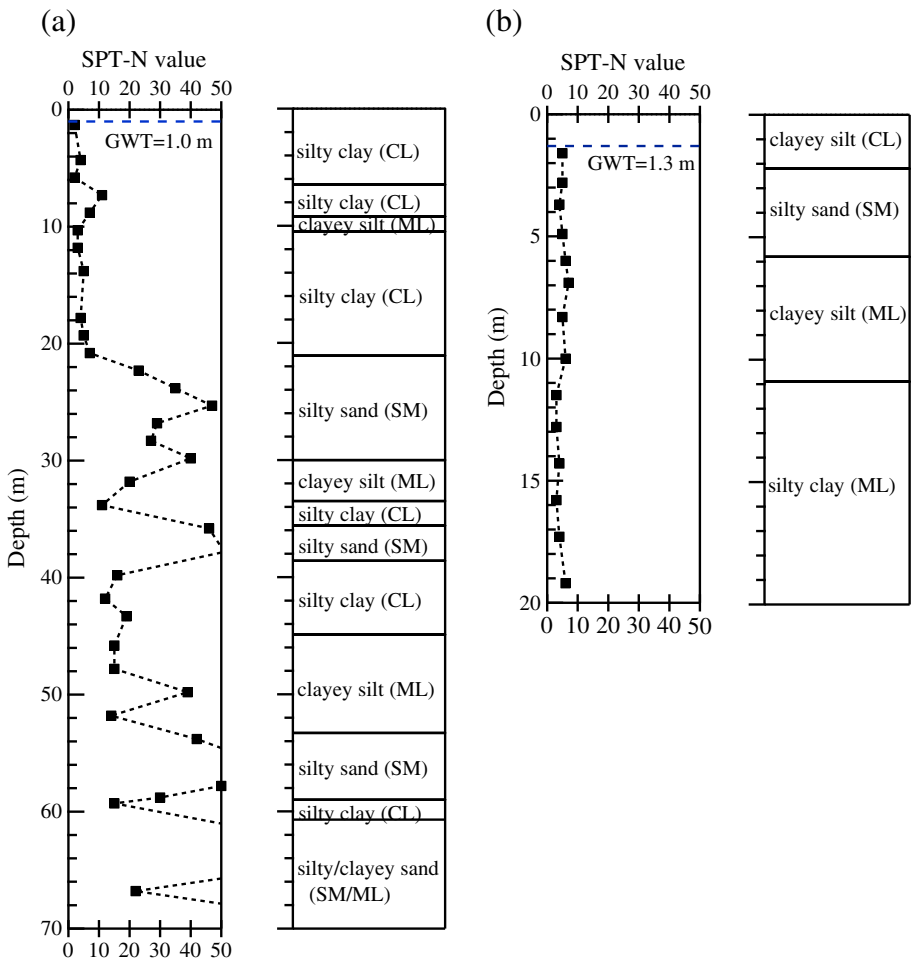

Fig. 6. Pre-earthquake boring logs: (a) THSR-BH24, and (b) CECI-BH04.

4.3. Shear wave velocity profile

Two in situ shear wave velocity measurement techniques, including multichannel analysis of surface waves (MASW, Park et al., 1999) and downhole tests during the CPT penetration process (SCPT), are employed in this investigation for cross verifications. The MASW was performed three days after the earthquake using a 12 lb sledge hammer and a rubber strike plate as the energy source, which resulted in sampling depth down to 11 m. The downhole tests were performed during the CPT penetration at 1 m intervals down to 22 m deep. The downhole seismic data were processed with an interval downhole method and the results represent the average shear wave velocity (V_s) between two measuring depths.

The V_s profiles from both techniques are plotted in Fig. 9 along with the soil layers from the borehole log of SLS. The results show that the V_s profiles from both techniques are very consistent for the top 10 m of soils, indicating the high confidence of the testing data. The MASW results also show that the ground water table was at 0.4 m deep three days after the earthquake. Based on the Vs profile, the shear wave velocity of the silty sand layer is 120 to 150 m/s after the earthquake, which indicates that liquefaction could be easily triggered based on correlations by Andrus and Stokoe (2000).

4.4. Laboratory testing

To evaluate the liquefaction potential with different techniques, laboratory tests for soil physical properties, dynamic soil properties, and liquefaction resistance of the liquefied stratum were conducted. The grain size distribution tests were conducted on ejected soils collected from sand boil deposits and split tube samplers from the liquefied soil layer. The grain size distribution curves of the ejected soil and silty sands at depths of 5 and 8 m are plotted in Fig. 10. The grain size analysis shows that the grain size distribution of the ejected soil is close to the two curves from the silty sand layer at depths from 4 to 9 m and the D_{50} of the liquefied soil is 0.09 mm. Visual inspection also shows that both the ejected soil and the silty sand are angular to subangular fine sand with grey color. From the soil color, shape, grain size distribution, and soil classification of the ejected soil and the silty fine sand, it confirms that the silty sand layer at depths from 4 to 8 m did liquefy during the Jiasian earthquake.

To directly evaluate the liquefaction resistance of the liquefied silty fine sand, cyclic direct simple shear tests under K_0-condition (K_0-CDSS) were performed on undisturbed specimens retrieved at depths from 5 to 6 m. To reduce the disturbance during sampling process, a gel-push sampler was used and V_s of specimen was measured to assess the quality of soil samples. The gel-push sampler developed in Japan (Tani and Kaneko, 2006) was modified from a 75 mm Osterberg piston sampler. Huang et al. (2008) reported the use of a gel-push sampler to recover high quality samples in silty sands at a test site in Southern Taiwan, where the fines contents varied from 5 to over 60%. Their results indicate that the laboratory V_s falls within or close to the range of those from SCPT at comparable depths. The same crew and equipment is employed to operate the gel-push sampler in this investigation and the V_s of specimens consolidated to the field vertical effective stress (~55 kPa) ranged from 135 to 145 m/s, which is within the range of in situ V_s from MASW and SCPT. The V_s

Table 2
Post-earthquake borehole data.

Depth (m)	Soil description	SPT-N	Sand (%)	Silt (%)	Clay (%)	USCS	PI (%)	γ (t/m^3)
1	yellow silty clay 1.3 m	5	11	45	44	CL	10	1.97
2	yellow silty fine sand 2.9 m	4	23	52	25	ML	NP	1.78
3		2	23	57	20	ML	NP	1.85
4	grey silty clay 3.4 m	7	46	40	14	ML	NP	2.00
5	grey silty fine sand with	3	70	27	3	SM	NP	1.83
6	silt seams 8.1 m	6	54	43	3	SM	NP	1.98
7		9	72	23	5	SM	NP	1.87
8		12	81	15	4	SM	NP	1.91
9	grey silty fine sand 9.0 m	4	77	19	4	SM	NP	1.79
10	grey silty clay with silt	4	2	54	44	CL	12	1.78
11	seams 10.7 m	4	1	54	45	CL-ML	5	1.89
12	grey silty clay 11.9 m	7	2	54	44	CL	8	1.87
13	grey silty clay with silt	5	14	46	40	CL	14	2.05
14	seams 20.0 m	3	6	54	40	CL	13	1.83
15		3	12	53	35	CL	12	1.82
16		5	7	50	43	CL	22	1.78
17		5	4	58	38	CL-ML	5	1.97
18		5	1	48	51	CL	11	1.90
19		7	1	51	48	CL	12	2.04
20		6	1	51	48	CL	14	1.97
21	grey silty fine sand	37	72	23	5	SM	–	1.91
22	~30.0 m	32	85	10	5	SM	–	1.87
23		53	61	34	5	SM	–	1.89
24		62	67	28	5	SM	–	2.01
25		64	63	32	5	SM	–	2.02
26		42	60	35	5	SM	–	1.96

Note: 1. Ground water table at 1.4 m below surface.
2. Silt defined as grain size between 5 and 75 μm.
3. Clay defined as grain size smaller than 5 μm.

comparison between the field and laboratory soils indicates that the disturbance from sampling and specimen preparation process is insignificant.

The K_0-CDSS system uses a circular soil container consisted with a latex membrane reinforced with stack rings to maintain the K_0 condition, defined as non-lateral expansion when subjected vertical loading. The testing procedure combined the ASTM D5311-92 (triaxial liquefaction potential testing) and D6528-07 (consolidated undrained direct simple shear testing) standards. After the completion of saturation, an effective vertical stress (σ'_{vo}) of 55 kPa was applied on specimens for consolidation, and this replicated the in situ stress conditions. A sinusoidal shear stress with a constant stress amplitude at a shearing frequency of 0.1 Hz was applied on specimens in an undrained condition until the soil reached initial liquefaction, defined as 100% excess pore pressure ratio r_u ($r_u = \Delta u/\sigma'_{vo}$, Δu = excess pore pressure) or a shear strain level in excess of 3.75%. Due to the high fines content, the initial liquefaction of the silty fine sand is defined on the shear strain level criteria. The liquefaction resistance test results in terms of the cyclic stress ratio ($CSR = \tau/\sigma'_{vo}$, τ = shear stress amplitude) and number of cycles to trigger initial liquefaction are plotted in Fig. 11. Following the magnitude-duration correlation proposed by Seed and Idriss (1982), the cyclic resistance resistances for $M_w = 7.5$ ($N_L = 15$ cycles) and $M_w = 6.4$ ($N_L = 6$ cycles) are 0.137 and 0.152, respectively.

Dynamic soil properties represented as modulus reduction and damping curves are important parameters when performing site specific response analysis and advanced dynamic analysis. To establish the variations of secant shear modulus and damping ratio at different shear strain levels, resonant column (RC) and K_0-CDSS tests were performed on undisturbed specimens. The resonant column test was performed under an isotropic consolidation stress, but the K_0-CDSS was tested under an anisotropic consolidation stress. To reduce the effect from different confining stresses, the variations of shear modulus with shear strain amplitude (γ) are presented as normalized modulus, which is defined as the shear modulus at different shear strain amplitudes ($G(\gamma)$) divided by the maximum shear modulus (G_{max}), defined as the shear modulus at shear strain levels of less than 10^{-4}%. For the resonant column test, the maximum shear strain amplitude is up to 10^{-2}%. For the K_0-CDSS test, the shear strain amplitude ranges from 5.5×10^{-2} to 10%, and the G_{max} was evaluated using integrated bender elements. The normalized modulus reduction curves for soil at depths of 5 to 6 m are plotted in Fig. 12(a), along with the mean and upper bound curves for sandy soil by Seed and Idriss (1970). In addition, the results for silty fine sand soil fit well to the modified hyperbolic relationship proposed by Hardin and Drenvich (1972) with reference shear strain (γ_r) of 0.045. The damping ratios of the test data and the mean and lower bound curves

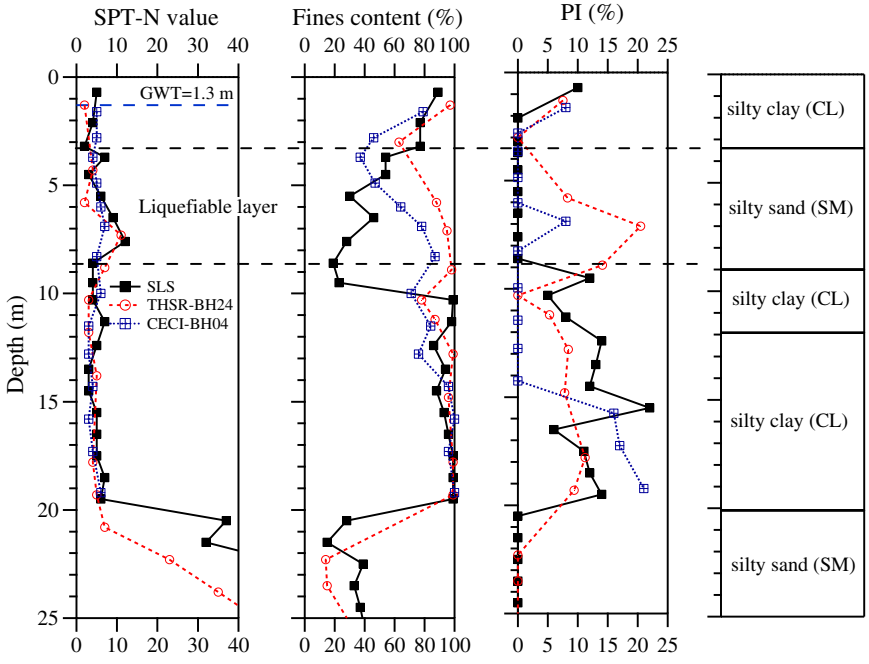

Fig. 7. Compiled borehole logs and soil layers.

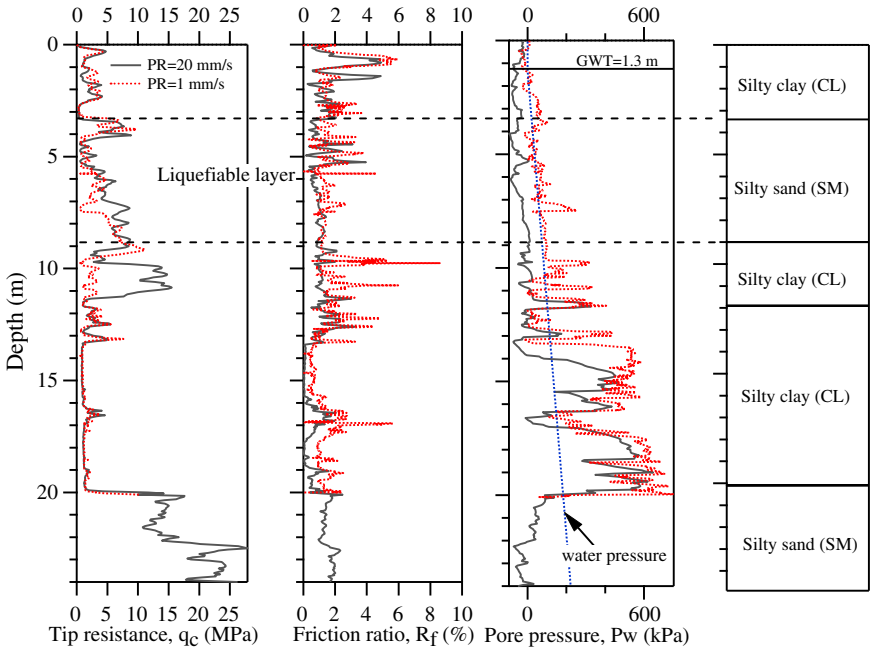

Fig. 8. Post-earthquake CPT soundings.

by Seed and Idriss (1970) are plotted in Fig. 12(b). In general, the liquefied soil falls within the typical curves for sand by Seed and Idriss (1970). Incorporating the Vs shown in Fig. 9, where V_s at 5 to 6 m deep is 143 to 148 m/s, the modulus reduction relationship can be inferred and used in the advanced ground response analyses and liquefaction evaluations.

5. Liquefaction analysis

The SPT, CPT, V_s, and laboratory testing data were used to evaluate the liquefaction susceptibility before and after the Jiasian earthquake at Sinhua site. The semi-empirical procedure outlined by Idriss and Boulanger (2006) was used to evaluate the liquefaction potential in terms of the cyclic stress ratio induced by the earthquake (CSR) and the cyclic resistance ratio (CRR), which represents the capacity of soil against liquefaction. The CSR is evaluated as:

$$CSR = \frac{\tau}{\sigma'_{vo}} = 0.65\frac{a_{\max}}{g}\frac{\sigma_{v0}}{\sigma'_{vo}}r_d \quad (2)$$

where τ is the average shear stress, $a_{\max}$ is the maximum horizontal acceleration at the ground surface, g is the gravitational acceleration, σ_{vo} and σ'_{vo} are the total and effective vertical stress, respectively, and r_d is the stress reduction coefficient. The liquefaction susceptibility criteria for silts and clays proposed by Boulanger and Idriss (2006) are applied to distinguish the sand-like and clay-like soils based on the PI value.

Three semi-empirical correlations were employed to evaluate the CRR for a magnitude of $M_w = 7.5$ ($CRR_{7.5}$). The correlations between the $CRR_{7.5}$ and corrected SPT-N value ($N_{1,60}$) by Idriss and Boulanger (2006), the $CRR_{7.5}$ and normalized corrected cone resistance (Q_{tn}) by Robertson (2009), and the $CRR_{7.5}$ and overburden-stress corrected shear wave velocity (V_{s1}) by Andrus and Stokoe (2000) are used in this study. A magnitude scaling factor (MSF) is

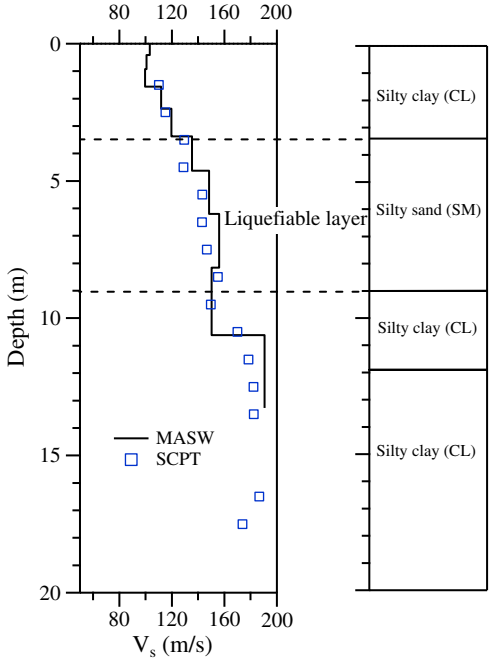

Fig. 9. Post-earthquake V_s profiles at Sinhua site.

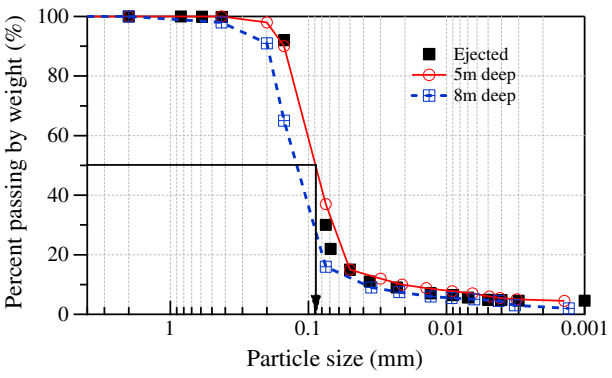

Fig. 10. Grain size distributions of ejected material and split tube samples.

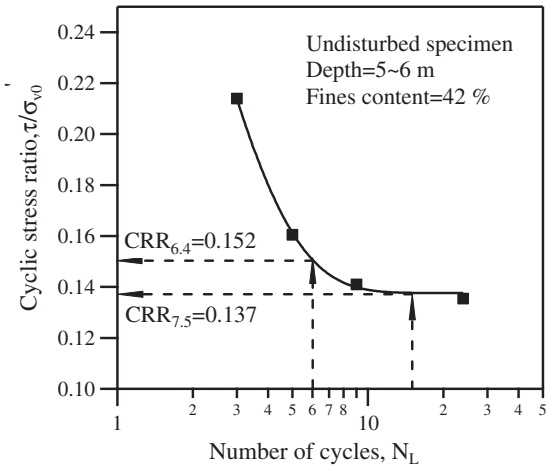

Fig. 11. Liquefaction resistance of undisturbed specimen by K_0-CDSS test.

applied to evaluate the CRR for earthquake magnitude M (CRR_M) by:

$$CRR_M = CRR_{7.5} \times MSF \tag{3}$$

A factor of safety against liquefaction (FS_{LF}), defined as the ratio between CRR and CSR, of less than 1.0 indicates that the soil could liquefy.

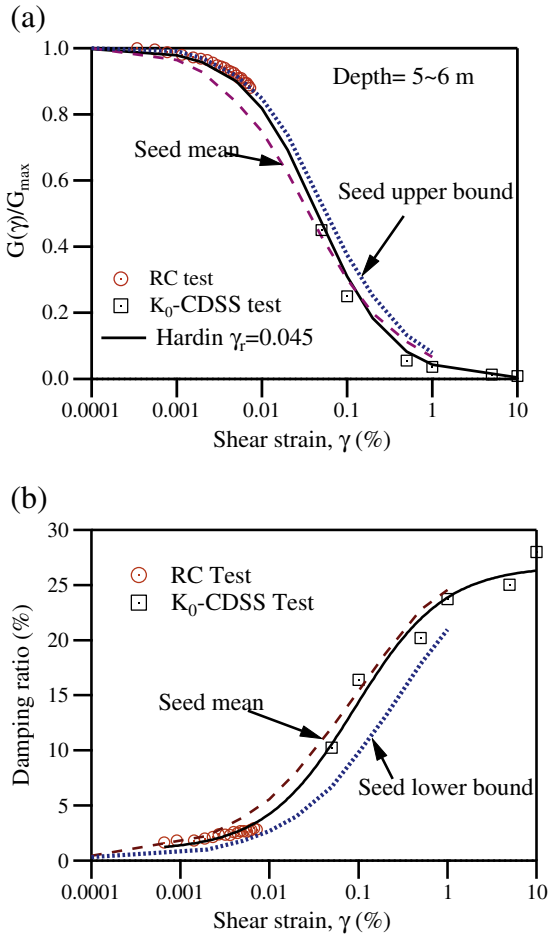

Fig. 12. Dynamic soil properties of Sinhua site at depths of 5 to 6 m: (a) normalized modulus reduction curve, and (b) damping curve.

For the Sinhua site subjected to the 2010 Jiasian earthquake, the a_{max} is 0.189 g (geometric mean of two horizontal components) and the M_w is 6.4, which corresponds to a magnitude scaling factor of 1.34 (Idriss and Boulanger, 2006). When computing the factor of safety against liquefaction (FS_{LF}) with CRR-$N_{1,60}$ curve, the soil layers with PI > 7 and soils deeper than 20 m were considered non-liquefied soil layers. As a result, liquefaction analyses were only performed for the silty sand layer at depths from 4 to 9 m.

The revised $CRR_{7.5}$-($N_{1,60}$) relationship, fines content correction, and overburden correction factor by Idriss and Boulanger (2006) are used to evaluation the pre- and post-earthquake CRR corresponding to Jiasian earthquake with CECI-BH04 and SLS boring log, respectively, and the results are shown in Fig. 13. Pre-earthquake analysis shows that the critical layer is located at depths from 4 to 6 m with fines content of 37 to 64%. The post-liquefaction analysis indicates that liquefaction could occur only at depths from 5 to 6 m. The post-earthquake liquefaction analysis with the curve of $CRR_{7.5}$-V_{s1} by Andrus and Stokoe (2000) is also plotted in Fig. 13 and it indicates that soil liquefaction could occur at depths from 4 to 9 m.

The normalized cone parameter (Q_{tn}) recommended by Robertson (2009) is implemented to assess the liquefaction resistance with the two CPT soundings and the results are plotted in Fig. 14. The soil behavior type index (I_c) values of 2.5 and 2.7 are plotted to represent the drained, partially drained, and undrained conditions during penetration. The results from the CPT sounding with slow penetration rate (PR = 1 mm/s) indicates that soil could liquefy at depths from 4.5 to 7 m. However, the results from the CPT sounding with standard penetration rate (PR = 20 mm/s) shows that the factor of safety is greater than 1 at the depth of 5.2 m due to high I_c value ($I_c = 2.79$). The adverse results from the two CPT soundings with different penetration rates indicate that drainage condition during penetration should be carefully treated for high fines content soil in the liquefaction analysis.

The outcomes of liquefaction potential evaluation with pre- and post-earthquake in situ index properties show that the critical layer is located at depths from 5 to 6 m for the Jiasian earthquake. To test the performance of different semi-empirical correlations on silty fine sands with high fines content in this area, comparisons of cyclic resistances from different in situ testing techniques and laboratory K_0-CDSS on undisturbed specimens are conducted. To make fair comparisons, the laboratory $CRR_{7.5}$ from K_0-CDSS is multiplied with a factor of 0.9 to take into account of the multidirectional shaking effects as proposed by Seed (1979). The average values of $CRR_{7.5}$ evaluated from in situ testing at depths from 5 to 6 m are presented in Table 3. In addition to the abovementioned correlations, the boundary curve of $CRR_{7.5}$-(q_c/V_s) for Holocene soils proposed by Roy (2008) is also included in the comparisons. The comparisons show that $CRR_{7.5}$ by CPT with standard penetration rate is overestimated in this silty fine sand layer due to high I_c value. Additionally, the variations of CRRs from different in situ tests indicate that those correlations are soil specific as addressed by Baxter et al. (2008) and precautions should be taken when using these on silty fine sand layers.

6. Summary and conclusion

This paper presents the comprehensive geotechnical reconnaissance of a liquefaction site at a Quaternary alluvial deposit in southern Taiwan. Liquefaction was triggered by a $M_w = 6.4$ earthquake about 44 km away at a silty fine sand layer located at depths of 5 to 6 m with $D_{50} = 0.09$ mm and fines content greater than 35%. The recurrence of liquefaction, influence of dynamic soil-structure interaction on triggering liquefaction, availability of pre-earthquake logging, and high fine content in the liquefied soil stratum make this case valuable for detail study. Subsurface characterizations, including SPT, CPT, V_s, and K_0-CDSS tests on undisturbed specimens retrieved

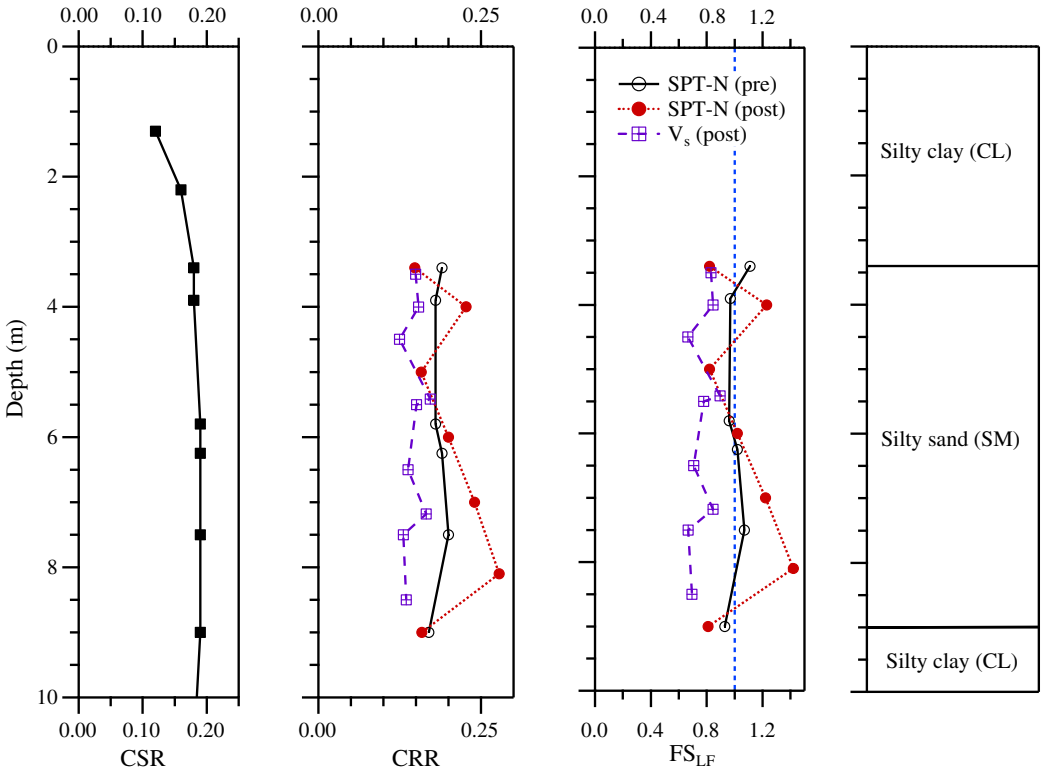

Fig. 13. Liquefaction analyses results with SPT-N and V_s at Sinhua site.

with a modified hydraulic piston sampler, were performed to establish a comprehensive case history for liquefaction study.

The grain size distribution and visual color of the ejected soil, back-calculated liquefaction potential with a pre-earthquake boring log, and post-earthquake boring log show that the silty sand layer at depths from 5 to 6 m liquefied during the 2010 Jiasian earthquake. Comparisons between the pre- and post-earthquake boring logs indicate that the average SPT-N values in the liquefiable silty fine sand layer (4–9 m) increased from 5 to 7.5 and the average fines content reduced from 60 to 35% after liquefaction. The results show that liquefaction could change the soil properties in silty fine sand interlayer at Sinhua site.

The revised simplified procedure by Idriss and Boulanger (2006) is used in evaluating the CSR and CRR from SPT-N values. Pre-earthquake analysis confirms that soil at depths from 5 to 6 m liquefied during the Jiasian earthquake. Liquefaction resistances from post-earthquake

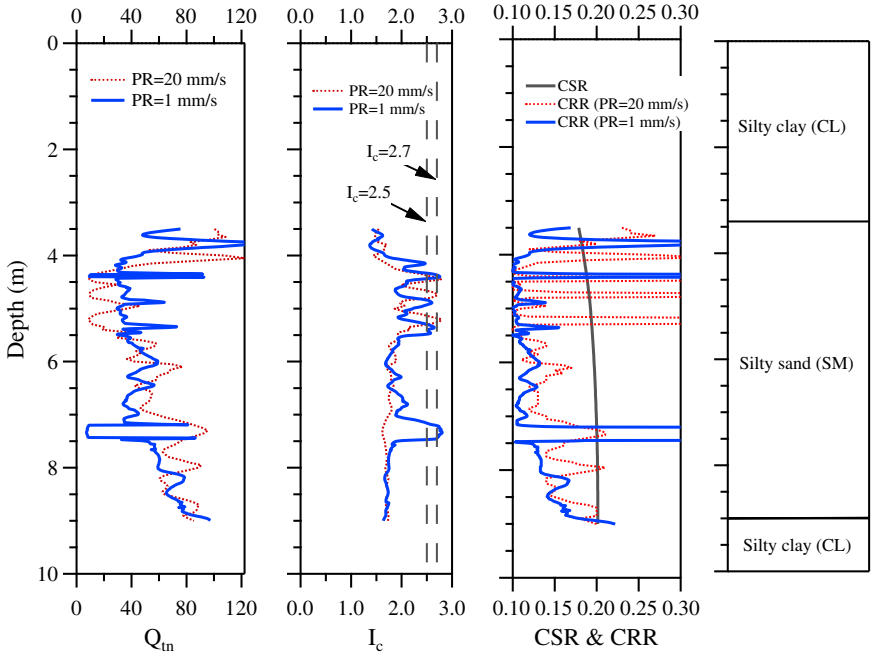

Fig. 14. Liquefaction analyses of CPT soundings at Sinhua site.

Table 3
Comparison of $CRR_{7.5}$ at depths of 5–6 m in Sinhua Site.

Method	$CRR_{7.5}$	$\frac{CRR_{in-situ}}{CRR_{lab}}$	Reference
K_0-CDSS	0.123	1	Seed (1979)
SPT-N	0.12	0.98	Idriss and Boulanger (2006)
CPT (PR = 20 mm/s)	0.131	1.06	Robertson (2009)
CPT (PR = 1 mm/s)	0.09	0.73	Robertson (2009)
V_s	0.1	0.81	Andrus and Stokoe (2000)
q_c/V_s	0.075	0.61	Roy (2008)

in situ tests, including SPT, CPT with two penetration rates, and V_s measurement, are evaluated for the liquefied silty fine sand layer at depths from 5 to 6 m and the results are compared with laboratory K_0-CDSS tests on undisturbed specimens. The cyclic resistances from the two CPT soundings show that $CRR_{7.5}$ by CPT with standard penetration rate could be overestimated in this silty fine sand layer due to high I_c value and the drainage condition during penetration should be considered for high fines content soil in the liquefaction analysis. Additionally, variations of CRRs from different in situ tests indicate that correlations among CRR and in situ tests could be soil specific and precautions should be taken when using these curves on silty fine sand layers. Nevertheless, liquefaction analyses with in situ test data and laboratory results show that this site is still highly susceptible to liquefaction.

Acknowledgements

This study was supported by the National Science Council, Taiwan, ROC, under grant No. NSC 98-2211-E-260-029. The authors are also grateful for the graduate students at NCKU for conducting the laboratory work. Any opinions, findings, and conclusions or recommendations expressed in this material are those of the authors, and do not necessarily reflect the views of the National Science Council.

References

Andrus, R.D., Stokoe II, K.H., 2000. Liquefaction resistance of soils from shear-wave velocity. Journal of Geotechnical and Geoenvironmental Engineering, ASCE 126 (11), 1015–1025.
Baxter, C.D.P., Bradshaw, A.S., Green, R.A., Wang, J.H., 2008. Correlation between cyclic resistance and shear-wave velocity for Providence silts. Journal of Geotechnical and Geoenvironmental Engineering, ASCE 134 (1), 37–46.
Boulanger, R.W., Idriss, I.M., 2006. Liquefaction susceptibility criteria for silts and clays. Journal of Geotechnical and Geoenvironmental Engineering, ASCE 132 (11), 1413–1426.
Central Geological Survey, MOEA, 2005. Geologic map of Taiwan: Shinhua sheet.
Central Geological Survey, 2010. MOEA, Taiwan. http://www.moeacgs.gov.tw/.
Chang, L.S., Chow, M.C., Chen, P.Y., 1947. The Tainan earthquake of December 5, 1946. Bulletin of Geological Survey, Taiwan 1, 11–18.
Hardin, B.O., Drenvich, V.P., 1972. Shear modulus and damping in soils: design equations and curves. Journal of the Soil Mechanics and Foundations Division, ASCE 98 (SM7), 667–692.
Huang, A.B., Tai, Y.Y., Lee, W.F., Ishihara, K., 2008. Sampling and field characterization of the silty sand in Central and Southern Taiwan. Proc. 3rd International Conference on Site Characterization (ISC-3). Taylor and Francis, Taipei, pp. 1457–1463.
Idriss, I.M., Boulanger, R.W., 2006. Semi-empirical procedures for evaluating liquefaction potential during earthquakes. Soil Dynamics and Earthquake Engineering 26 (2–4), 115–130.
Kim, K., Prezzi, M., Salgado, R., Lee, W., 2008. Effect of penetration rate on cone penetration resistance in saturated clayey soils. Journal of Geotechnical and Geoenvironmental Engineering, ASCE 134 (8), 1142–1153.
Lee, S.J., Lui, S., 2010. 2010/03/04 M6.4 earthquake, Taiwan Finite-fault source rupture process: preliminary result. http://www.earth.sinica.edu.tw/~sjlee/eq20100304/index_e.htm.
Moh and Associates, 2000. Site investigation of liquefied soil at Nantou and Wufeng areas. (in Chinese).
Park, C.B., Miller, R.D., Xia, J., 1999. Multichannel analysis of surface waves. Geophysics 64 (3), 800–808.
Robertson, P.K., 2009. Performance based earthquake design using the CPT. Proc., IS Tokyo Conf. CRC Press/Balkema, Taylor and Francis Group, Tokyo.
Roy, D., 2008. Coupled use of cone tip resistance and small strain shear modulus to assess liquefaction potential. Journal of Geotechnical and Geoenvironmental Engineering, ASCE 134 (4), 519–530.
Seed, H.B., 1979. Soil liquefaction and cyclic mobility evaluation for level ground during earthquakes. Journal of the Geotechnical Engineering Division, ASCE 105 (2), 201–255.
Seed, H.B., Idriss, I.M., 1970. Soil moduli and damping factors for dynamic response analyses. Report EERC 70–10. Earthquake Engineering Research Center, University of California, Berkeley.
Seed, H.B., Idriss, I.M., 1982. Ground motions and soil liquefaction during earthquakes. Earthquake Engineering Research Institute, Berkeley, California.
Tani, K., Kaneko, S., 2006. Method of recovering undisturbed samples using water-soluble thick polymer (in Japanese) Tsuchi-to-Kiso, Journal of Japanese Geotechnical Society 54 (4), 145–148.